PROCEEDINGS of the
23rd International Congress on Acoustics
9 to 13 September 2019 in Aachen, Germany

Evaluating acoustic properties based on sound energy for interior problems

Caglar GUERBUEZ[(1)], Steffen MARBURG[(1)]

[(1)]Chair of Vibroacoustics of Vehicles and Machines, Technical University of Munich, Germany, caglar.guerbuez@tum.de

Abstract

The analysis of sound radiation of vibrating structures is of great importance in order to develop low-noise emitting structures. For exterior problems, it was shown that the non-negative intensities shall be considered in order to evaluate the acoustic properties of a structure, since using this method accounts for the acoustic short circuit. This acoustic short circuit is a phenomenon which is present when evaluating the sound intensity of a structure. Regarding interior problems, the sound pressure level is commonly analyzed to characterize the acoustic behavior. However, the sound pressure level is strongly dependent on the position of the field point of interest. Thus, the analysis of the sound pressure level is highly sensitive to deviations of the field point position. This paper introduces the sound energy as an appropriate quality criteria for interior problems due to the global characteristic. The sound energies are compared with the sound pressure level for numerical benchmark examples and real world applications. Based on the time harmonic problem formulation, the acoustic interior problem is solved with the boundary element method (BEM).

Keywords: Acoustic Radiation, Interior Problem, Boundary Element Method, Sound Energy

1 INTRODUCTION

For exterior problems, the non-negative intensity (NNI) is an appropriate quality criterion since it circumvents the effect of the acoustic short circuit [11]. The formulation of the NNI is derived by the acoustic radiation modes which are obtained by the eigenvalue analysis of the impendance matrix [13]. Based on the NNI, the surfaces which are contributing to the sound power can be identified [3, 11]. Unfortunately, the NNI is not suitable for interior problems because of the near-field and reflection effects which are present in the interior problem [2]. Nevertheless, this motivates an energy-based approach which is suitable for interior problems. Usually, interior problems are analyzed by evaluating the sound pressure level at several field points. This makes the sound field evaluation strongly sensitive to deviations of the field point position. In order to avoid the problem of the locality, Koopmann and Fahnline [2] introduce sound energies as an appropriate quality criterion. As a global acoustic quantity, the sound energies are unaffected by field point deviations, whilst they preserve the acoustic behavior of an enclosure.

Based on a BEM discretization, this contribution deals with the evaluation of the sound energy as an appropriate quality criterion. It will be compared with the sound field evaluation considering a numerical benchmark example and an application of the automotive industry, e.g. the acoustic behavior of a sedan cabin compartment.

2 BOUNDARY ELEMENT METHOD

In this contribution, the derivation of the boundary element method (BEM) is presented only in a condensed form. The presentation of the BEM is reduced to the main equations and assumptions which are relevant for this paper. For a comprehensive and detailed description, the interested reader is referred to the lecture notes [12]

2.1 Helmholtz equation and boundary integral equation

Considering the time-harmonic scalar wave equation for the sound pressure p in a bounded domain $\Omega \subset \mathbb{R}^3$ with the boundary $\Gamma = \partial\Omega$ and the unit normal vector $\boldsymbol{n}$ outward to Ω, the Helmholtz equation for acoustic

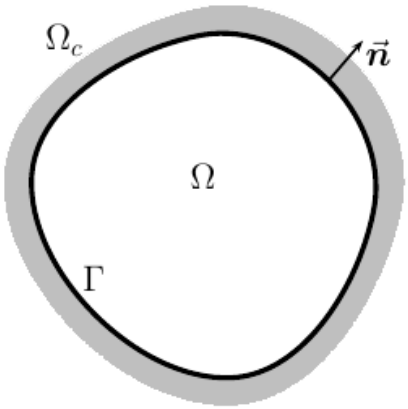

Figure 1. Definition of the interior problem with the domain Ω and its complementary Ω_c. The unit normal $\boldsymbol{n}$ on the boundary Γ points outward to Ω.

radiation problems can be expressed as

$$\Delta p(\boldsymbol{x}) + k^2 p(\boldsymbol{x}) = 0 \qquad \text{with} \quad \boldsymbol{x} \in \Omega \subset \mathbb{R}^3 \tag{1}$$

with $k = \omega/c$ as the wavenumber. The wavenumber k is evaluated by the angular frequency ω and the speed of sound c. In Figure 1, the acoustic interior problem is depicted.

The Helmholtz equation satisfies the boundary conditions on Γ as well as the Sommerfeld radiation condition at infinity. The boundary condition on Γ is equivalent to a Robin boundary condition which results into a boundary condition of Neumann type for zero admittance. The Robin boundary condition is defined as

$$v_f(\boldsymbol{x}) - v_s(\boldsymbol{x}) = Y(\boldsymbol{x}) p(\boldsymbol{x}) \qquad \text{with} \quad \boldsymbol{x} \in \Gamma \subset \mathbb{R}^2 \tag{2}$$

with Y representing the boundary admittance. The boundary admittance establishes the relation between the sound pressure p and the difference of the fluid particle velocity v_f and the structural particle velocity v_s in normal direction. By means of the linearized Euler equation, the fluid particle velocity in normal direction can be expressed by the derivative of the sound pressure in normal direction

$$v_f(\boldsymbol{x}) = \frac{1}{i\rho\omega} \frac{\partial p(\boldsymbol{x})}{\partial n(\boldsymbol{x})} \tag{3}$$

with ρ as the ambient density of the fluid and i the imaginary unit. The method of weighted residuals regarding the Green's function for the test function results into the Kirchhoff-Helmholtz integral equation. Incorporating the admittance boundary condition, the associated boundary integral equation reads

$$c(\boldsymbol{y}) p(\boldsymbol{y}) + \int_\Gamma \left[\frac{\partial G(\boldsymbol{x},\boldsymbol{y})}{\partial \boldsymbol{n}(\boldsymbol{x})} - i\omega\rho G(\boldsymbol{x},\boldsymbol{y}) Y(\boldsymbol{x}) \right] p(\boldsymbol{x}) d\Gamma(\boldsymbol{x}) = i\rho\omega \int_\Gamma G(\boldsymbol{x},\boldsymbol{y}) v_s(\boldsymbol{x}) d\Gamma(\boldsymbol{x}) \tag{4}$$

with the Green's function as

$$G(\boldsymbol{x},\boldsymbol{y}) = \frac{1}{4\pi} \frac{\mathrm{e}^{ikr(\boldsymbol{x},\boldsymbol{y})}}{r(\boldsymbol{x},\boldsymbol{y})} \tag{5}$$

where r is the Euclidean distance between the field point x and the source point y. The coefficient c represents the integral free term. The integral free term is $c = 0.5$ for y on a smooth surface which will be the case in the following numerical examples.

2.2 Collocation method

The boundary integral equation in Eq.(4) is discretized by testing it with delta functions. Moreover, the acoustic field quantities are approximated by the same Lagrangian interpolation polynomials $\boldsymbol{\varphi}$. The resulting linear system of equations can be then expressed by

$$(\boldsymbol{H} - \boldsymbol{GY})\boldsymbol{p} = \boldsymbol{Gv_s} \tag{6}$$

where the system matrices $\boldsymbol{G}$ and $\boldsymbol{H}$ are dense, complex valued and non-hermitian. In the numerical experiments, discontinuous Lagrangian elements with linear interpolation functions are applied. The system of equations in Eq.(6) is solved iteratively using a GMRes algorithm.

2.3 Field point evaluation and sound energies

Regarding the boundary data for the sound pressure and the particle velocity, one can obtain the sound pressure at an arbitrary field point. For this purpose, the boundary integral equation in Eq.(4) is rearranged for the field point $\boldsymbol{y} \in \Omega$

$$p(\boldsymbol{y}) = \int_\Gamma i\omega\rho G(\boldsymbol{x},\boldsymbol{y}) v_f(\boldsymbol{x}) d\Gamma(\boldsymbol{x}) - \int_\Gamma \frac{\partial G(\boldsymbol{x},\boldsymbol{y})}{\partial n(\boldsymbol{x})} p(\boldsymbol{x}) d\Gamma(\boldsymbol{x}). \tag{7}$$

The discretized version of Eq.(7) can be expressed as

$$p(\boldsymbol{y}) = \boldsymbol{g}^T(\boldsymbol{y})\boldsymbol{v}_f - \boldsymbol{h}^T(\boldsymbol{y})\boldsymbol{p} \tag{8}$$

with $\boldsymbol{p}$ and $\boldsymbol{v}_f$ as the nodal data for the sound pressure and the particle velocity, respectively. The data in the column matrices $\boldsymbol{g}$ and $\boldsymbol{h}$ is evaluated as rows of the system matrices $\boldsymbol{G}$ and $\boldsymbol{H}$ with the field point replacing the collocation point

$$g_j(\boldsymbol{y}) = i\omega\rho \int_\Gamma G(\boldsymbol{x},\boldsymbol{y}) \varphi_j(\boldsymbol{x}) d\Gamma(\boldsymbol{x}), \tag{9}$$

and

$$h_j(\boldsymbol{y}) = \int_\Gamma \frac{\partial G(\boldsymbol{x},\boldsymbol{y})}{\partial n(\boldsymbol{x})} \varphi_j(\boldsymbol{x}) d\Gamma(\boldsymbol{x}). \tag{10}$$

The acoustic field quantities, e.g. sound pressure and fluid particle velocity, are strongly dependent on the position of the field point. Thus, the analysis of the sound pressure level will be highly sensitive to deviations of the field point position. Koopmann and Fahnline introduce sound energies as an appropriate quality criterion for interior problems [2]. The total sound energy includes the potential energy and the kinetic energy. The potential energy describes the compression of the fluid particles and is evaluated by

$$E_p = \frac{1}{4\rho c^2} \int_\Omega |p(\boldsymbol{x})|^2 d\Omega(\boldsymbol{x}). \tag{11}$$

The kinetic energy, which comprises the motion of the fluid particles, can be expressed by

$$E_k = \frac{\rho}{4} \int_\Omega v(\boldsymbol{x}) \cdot v(\boldsymbol{x})^* d\Omega(\boldsymbol{x}). \tag{12}$$

The total energy E_{tot} can be then evaluated by

$$E_{tot} = E_p + E_k. \tag{13}$$

3 NUMERICAL EXAMPLES

Based on a BEM discretization, two numerical examples are considered in this contribution. Firstly, traveling and standing waves for long ducts are investigated. Secondly, an industrial application, e.g. sedan cabin compartment, is analyzed. In both examples, the sound pressure level at specific field points are compared with the sound energies.

3.1 Traveling and standing waves in long ducts

The first example is an air-filled duct as introduced in [1]. The duct has a length $L = 3.4\,\mathrm{m}$ and a square cross section $A = 0.04\,\mathrm{m}^2$. Moreover, the speed of sound and the ambient density are assumed to be $c = 343\,\mathrm{m/s}$ and $\rho = 1.21\,\mathrm{kg/m}^3$, respectively. Regarding the boundary conditions, a particle velocity is applied to one end, e.g. $v_s(x=0) = v_0$ with $v_0 = 1.0\,\mathrm{m/s}$, and an admittance boundary condition to the other end. In the first case, the standing waves are analyzed. Hence, the admittance boundary condition will be assumed to $Y_1(x=L) = 0$. In order to observe traveling waves, the admittance will be $Y_2(x=L) = 1/\rho c$. The duct is discretized with 140 linear, discontinuous elements where the nodes are positioned at the zeros of the Legendre polynomials. A schematic description of the first numerical example is depicted in Figure 2.

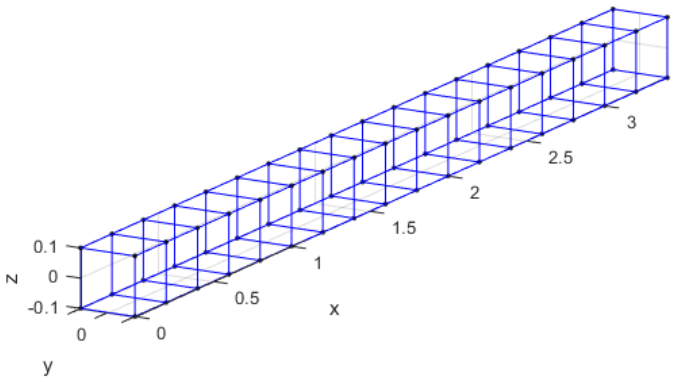

Figure 2. Schematic description of the duct example. The duct will be excited by a vibration at $x = 0$. The resulting waves are then fully reflected (first case, Y_1) or fully absorbed (second case, Y_2) at $x = L$.

In the following analyses, the potential energy E_p is firstly approximated by the mean sound pressure derived from a series of sound field evaluations

$$E_p \approx \frac{1}{4\rho c}\frac{1}{N}\sum_{k=1}^{N}|p(\boldsymbol{x})|^2. \tag{14}$$

The results of the sound pressure level at the field points and the potential energy are shown in Figure 3. In the analysis, the sound pressure level is evaluated at ten field points along the x-axis.

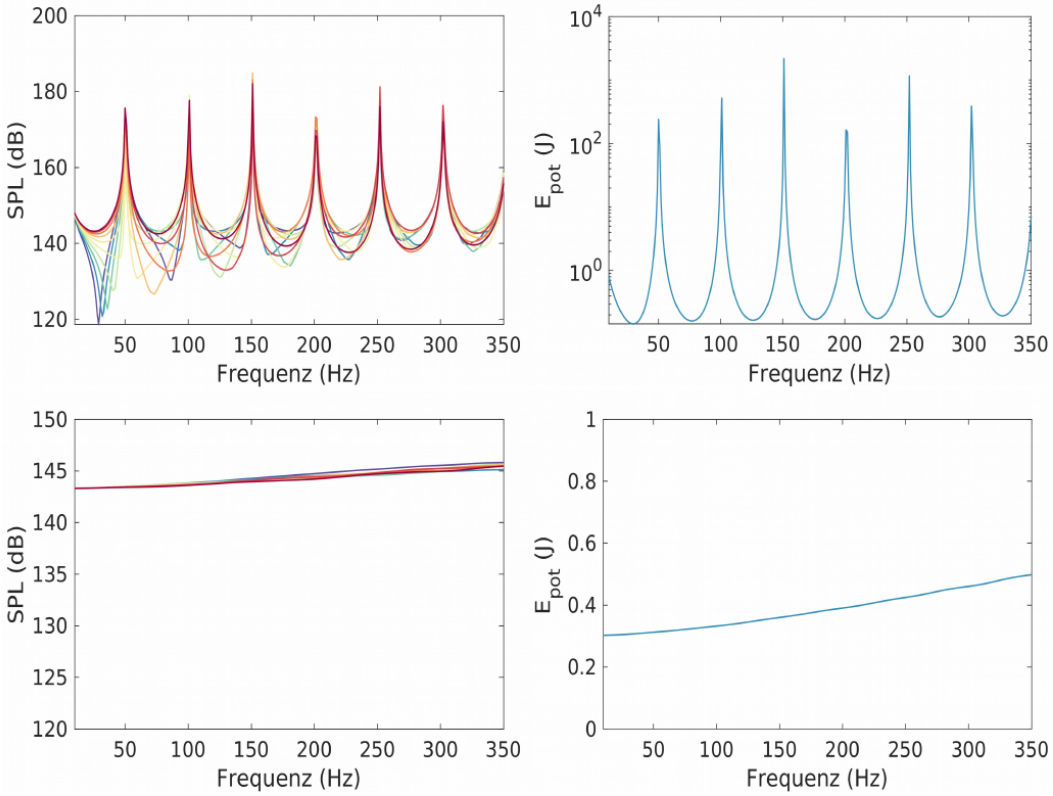

Figure 3. Sound radiation for the interior duct problem. In the upper row, the sound pressure level at several field points and potential energy are shown for zero boundary admittance, $Y_1 = 0$. The lower row depicts the results regarding a fully absorbing admittance boundary condition, $Y_2(x = L) = 1/\rho c$.

For standing waves (upper row), the results show that different field point position lead to different sound pressure levels. The potential energy however, represents the global characteristics of the standing waves without the deviations of the field points. In the lower row, the results for the traveling waves are depicted. Since the waves are fully absorbed at $x = L$, the deviations of the field points are nearly irrelevant. As in the case for the standing waves, the potential energy gathers the acoustic behavior in global sense.

3.2 Sedan cabin compartment

In addition to the duct problem, an industrial application, e.g. a sedan cabin compartment is investigated. Regarding the boundary conditions, a fictitious excitation excitation is realized by applying a particle velocity $v_s = 1.0\,\mathrm{m/s}$ at the lower left front area of the cavity. Moreover, a uniform boundary admittance of $Y = f/f_0\rho c$ with the reference frequency $f_0 = 2800\,\mathrm{Hz}$ is assumed at the surfaces of the cavity [9]. The mesh of the sedan cabin compartment is visualized in Figure 4.

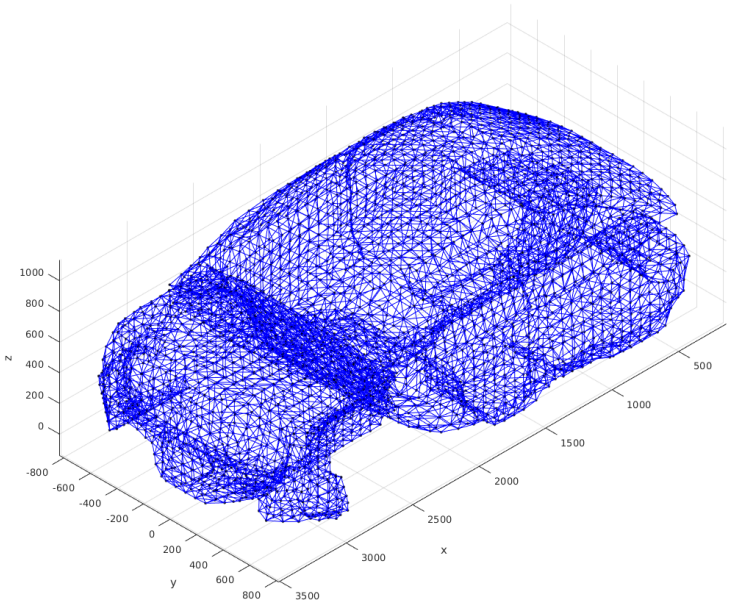

Figure 4. Mesh of the sedan cabin compartment.

4 CONCLUSIONS

This contribution introduces the sound energies as an appropriate quality criterion for interior acoustic problems. The sound pressure level, which is usually analyzed for interior problems, is highly sensitive to deviations of the field point position. On the contrary, the sound energy is unaffected by the deviations of the position, since it represents a global acoustic quantity. In this work, a numerical benchmark example, e.g. the duct example, and an application from the automotive industry were investigated. In these analyses, the sound pressure level was compared to the potential energy, which was capable of representing the global behavior of the underlying models without the dependencies on the field point positions. Future work will include the analysis of kinetic sound energy and the total sound energy. Moreover, the sound energy, which was approximately evaluated by the mean sound pressure of a series of sound field evaluations, needs to be computed for the entire domain. Since the analyses are performed with the BEM, the transformation of the volume integral into a surface integral, e.g. by the Gaussian divergence theorem, seems a promising approach.

REFERENCES

[1] Hornikx, M.; Kaltenbacher, M.; Marburg, S. A platform for benchmark cases in computational acoustics. Acta Acustica united with Acustica 101, 2015, pp. 811-820.

[2] Koopmann, G.; Fahnline, J. Designing quiet structures. A sound power minimization approach. Academic Press, San Diego, London, 1997, pp. 201-226.

[3] Liu, D.; Peters, H.; Marburg, S.; Kessisoglou, N. Supersonic intensity and non-negative intensity fo prediction of radiated sound power. The Journal of the Acoustic Society of America 139, 2016, pp. 2797-2806.

[4] Liu, D.; Peters, H.; Marburg, S.; Kessisoglou, N. Surface contributions to scattered sound power using non-negative intensity. The Journal of the Acoustic Society of America 140, 2016, pp. 1206-1217.

[5] Liu, D.; Havranek, Z.; Marburg, S.; Peters, H.; Kessisoglou, N. Non-negative intensity and back-calculated non-negative intensity for analysis of directional structure-borne sound. The Journal of the Acoustic Society of America 141, 2017, pp. 117-123.

[6] Marburg, S.; Hardtke, HJ. A study on the acoustic boundary admittance. Determination, results and consequences. Engineering Analysis with Boundary Elements 23, 1999, pp. 737-744.

[7] Marburg, S. Developments in structural-acoustic optimization for passive noise control. Archives of computational methods in engineering 9, 2002, pp. 291-370.

[8] Marburg, S. Efficient optimization of a noise transfer function by modification of a shell structure geometry-Part 1: Structural and Multidisciplinary Optimization 24, 2002, pp. 51-59.

[9] Marburg, S.; Hardtke, HJ. Investigation and optimization of a spare wheel well to reduce vehicle interior noise, Journal of Computational Acoustics 11, 2003, pp. 425-449.

[10] Marburg, S. How many elements per wavelength are necessary?, In: Marburg, S. and Nolte, B., editors, Computational Acoustics of Noise Propagation in Fluids. Finite and Boundary Element Methods, Springer, Berlin, 2008, pp. 309-332.

[11] Marburg, S.; Loesche, E.; Peters, H.; Kessissoglou, N. Surface contributions to radiated sound power, The Journal of the Acoustic Society of America, 2013, pp. 3700-3705.

[12] Marburg, S. Boundary element method for time-harmonic acoustic problems. In: M. Kaltenbacher, editor, Computational Acoustics, CISM International Centre for Mechanical Sciences, Courses and Lectures, Vol. 579, Springer, Berlin, Heidelberg, 2017, pp. 69-158.

[13] Peters, H.; Kessissoglou, N.; Marburg, S. Enforcing reciprocity in numerical analysis of acoustic radiation modes and sound power evaluation, Journal of Computational Acoustics, 2012, 1250005-1-19.

[14] Williams, E. Fourier Acoustics: Sound radiation and nearfield acoustical holography, Academic Press, London, 1999, pp. 67-77.